Bishexa-*peri*-hexabenzocoronenyl: A "Superbiphenyl"

Shunji Ito,[†] Peter Tobias Herwig,[†] Thilo Böhme,[‡] Jürgen P. Rabe,[‡] Wolfgang Rettig,[§] and Klaus Müllen*,[†]

Contribution from the Max-Planck-Institut für Polymerforschung, Ackermannweg 10, D-55128 Mainz, Germany, Institut für Physik, Humboldt Universität zu Berlin, Invalidenstrasse 110, D-10115 Berlin, Germany, and Institut für Chemie, Fach-Institut für Physikalische und Theoretische Chemie, Humboldt Universität zu Berlin, Bunsenstrasse 1, D-10117 Berlin, Germany

Received March 9, 2000

Abstract: The alkyl-substituted bishexa-*peri*-hexabenzocoronenyls **3a** and **3b** as well as the related alkyl-substituted dihexa-*peri*-hexabenzocoronenyldodecane **4** were synthesized. The good solubility of these compounds allowed a comprehensive spectroscopic characterization in solution. Both **3a** and **4** form liquid crystalline phases, while only in the case of **4** could a highly ordered columnar structure with a hexagonal superstructure be observed. Photophysical studies in solution revealed a strong intramolecular interaction of the aromatic cores of **3a**, in contrast to **4**, where only weak intramolecular interactions could be observed. Compound **3a** forms monomolecular adsorbate layers on graphite which were characterized by scanning tunneling microscopy.

Introduction

Hexa-*peri*-hexabenzocoronenes (HBCs, **1**) are readily available upon oxidative cyclodehydrogenation of the corresponding hexaphenylbenzene precursors.[1−3] Alkyl substitution is important to render HBC soluble in organic solvents. HBCs carrying *n*-alkyl substituents give rise to discotic mesophases over a broad temperature range[2] and prove as photoconductors with very high charge carrier mobilities.[4] Furthermore, they furnish monomolecular adsorbate layers on highly oriented pyrolytic graphite (HOPG) which can be characterized by scanning tunneling microscopy.[1] HBCs are also important electrophores and upon alkali metal reduction afford extended redox sequences ranging from the monoanions to the tetraanions.[5] It appears from solid-state ESR measurements that the charged anions possess high-spin states. This spin multiplicity is closely related to the possible degeneracy of HBC frontier orbitals, which follows from the hexagonal symmetry of the π-system. If from an electronic point of view HBC can thus be regarded as a homologue of benzene, i.e., as "superbenzene", it seems challenging to use HBC as a building block of more complex π-structures. As an example of an extensively fused polycyclic aromatic hydrocarbon (PAH),[6] we have recently synthesized "supernaphthalene" **2**[7] (see Chart 1).

Herein, we introduce the bishexa-*peri*-hexabenzocoronenyl **3** as an example of the "superbiphenyl" and the related dihexa-*peri*-hexabenzocoronenyldodecane **4** in which two HBC units are linked by a flexible alkyl chain. Compounds **3** and **4** are structural homologues of biphenyl **5** and 1,*n*-diphenylalkanes **6** together with their naphthalene and anthracene derivatives **7**−**10**.

Chart 1

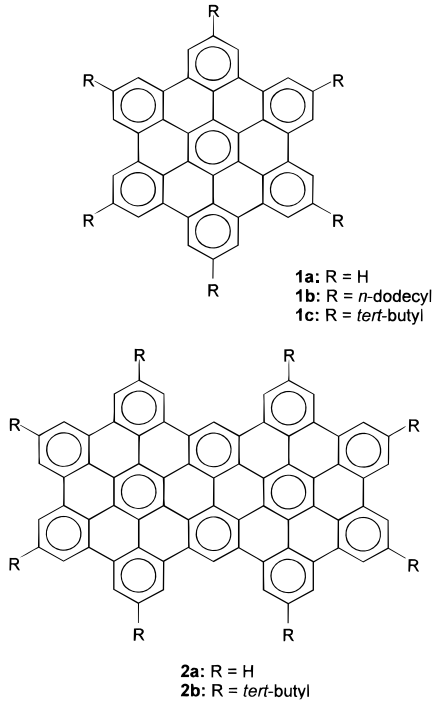

* Corresponding author: (fax) +49 6131 379 350; (e-mail) muellen@mpip-mainz.mpg.de.

[†] Max-Planck-Institut für Polymerforschung.

[‡] Institut für Physik, Humboldt Universität zu Berlin.

[§] Institut für Chemie, Humboldt Universität zu Berlin.

(1) Stabel, A.; Herwig, P.; Müllen, K.; Rabe, J. P. *Angew. Chem., Int. Ed. Engl*. **1995**, *34*, 1609. Müller, M.; Kübel, C.; Müllen, K. *Chem. Eur. J.* **1998**, *4*, 2099.

(2) Herwig, P.; Kayser, C. W.; Müllen, K.; Spiess, H. W. *Adv. Mater.* **1996**, *8*, 510.

(3) Herwig, P. T.; Enkelmann, V.; Schmelz, O.; Müllen, K. *Chem. Eur. J.*, in press.

(4) van de Craats, A. M.; Warman, J. M.; Müllen, K.; Geerts, Y.; Brand, J. D. *Adv. Mater.* **1998**, *10*, 36.

(5) Gherghel, L.; Brand, J. D.; Baumgarten, M.; Müllen, K. *J. Am. Chem. Soc.* **1999**, *121*, 8104.

(6) For further examples of extended polycyclic aromatic hydrocarbons, see: (a) Clar, E. *Aromatische Kohlenwasserstoffe-Polycyclische Systeme*; Springer, Berlin, 1952. (b) Clar, E. *The Aromatic Sextet*; Wiley: London, 1972. (c) Dias, J. R. *Handbook of Polycyclic Hydrocarbons-Part a: Benzenoid Hydrocarbons*; Elsevier: Amsterdam, 1987. (d) Fetzer, J. C. *Polycycl. Aromat. Comput.* **1996**, *11* (1−4), 317; (e) Diederich, F.; Rubin, Y. *Angew. Chem.* **1992**, *104*, 1123; *Angew. Chem., Int. Ed. Engl.* **1992**, *31*, 1101. (f) Hudgins, D. M.; Allamandola, L. J. *J. Phys. Chem.* **1995**, *99*, 3033. (g) Scott, L. T.; Cheng, P.-C.; Hashemi, M. M.; Bratcher, M. S.; Meyer, D. T.; Warren, H. B. *J. Am. Chem. Soc.* **1997**, *119*, 10963. (h) Faust, R. *Angew. Chem.* **1995**, *107*, 1559; *Angew. Chem., Int. Ed. Engl.* **1995**, *34*, 1429. (i) Müller, M.; Petersen, J.; Strohmaier, R.; Günther, C.; Karl, N.; Müllen, K. *Angew. Chem.* **1996**, *108*, 947; *Angew. Chem., Int. Ed. Engl.* **1996**, *35*, 886. (j) Tong, L.; Lau, H.; Ho, D. M.; Pascal, R. A., Jr. *J. Am. Chem. Soc.* **1998**, *120*, 6000. (k) Debad, J. D.; Bard, A. J. *J. Am. Chem. Soc.* **1998**, *120*, 2476.

10.1021/ja000850e CCC: $19.00
Published on Web 07/26/2000

Chart 2

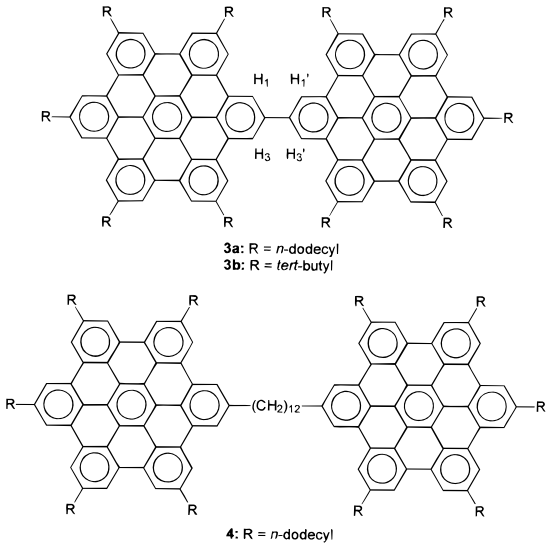

Chart 3

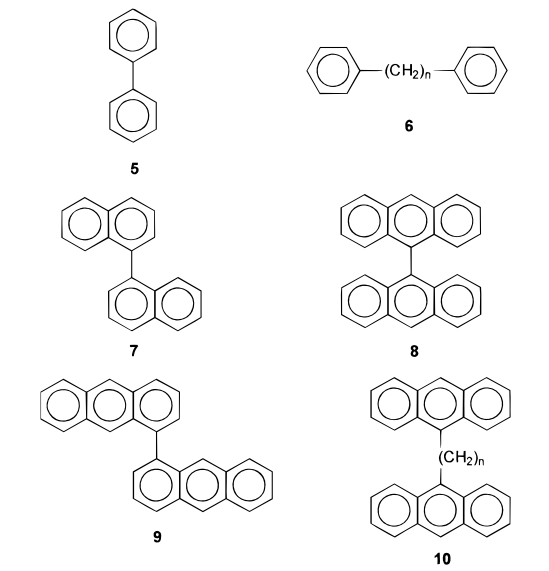

Not surprisingly, the solubilization of the title compounds **3** and **4** (Chart 2) requires alkyl substitution, where in the case of **3**, both the deca-*n*-dodecyl derivative **3a** and the deca-*tert*-butyl derivative **3b** were synthesized. It is remarkable that the new bis-HBCs **3a**, **3b**, and **4** are obtained from different routes where the key synthetic question is at what stage the hexaphenylbenzene precursor is transformed into the HBC disk.

Next to the synthetic challenge there are obvious structural reasons to investigate **3a** and **4**:

(1) Phase Formation. Oligomers consisting of rigid discotic cores interconnected directly or with flexible spacers are expected to display liquid crystalline order significantly different from that of the monomeric discotic cores. The bulk phase behavior of **3a** and **4** was therefore examined by polarizing microscopy, differential scanning calorimetry and X-ray diffractometry.

(2) Photophysical Properties. (i) The parent **1a** or **1b** has a 6-fold symmetry comparable to benzene, and it can be asked whether similar consequences such as a highly forbidden lowest singlet absorption and emission will be found.[8,9] (ii) The

Scheme 1. Synthesis of Bis-HBC's **3a** and **3b**[a]

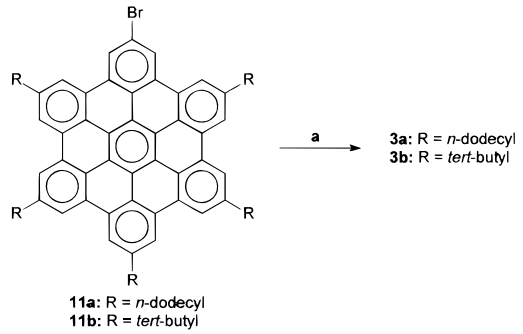

[a] Reaction conditions: (a) [Ni(COD)$_2$], COD, 2,2′-bipyridyl, toluene, 60 °C.

"superbiphenyl" **3a** can be compared with ordinary biphenyl or other biaryls in order to study the interaction between the two aromatic submoieties. (iii) Fluorescence spectroscopy is a very valuable and sensitive tool to discover the aggregation behavior of the species.

(3) Adsorption Layers. 3a can be considered as a soluble graphene segment. Adsorbed to graphite it serves as a model for small terraces or islands of graphite, which is of interest for a better understanding of the transition from molecular to solid-state electronic behavior in this class of materials. Extended polycyclic aromatic hydrocarbons such as **1**, **2**, and **3** can be regarded as 2D nanoparticles, which raises the exciting question of their single-molecule visualization and manipulation. This can finally lead to the use of single molecules as functional units in molecular electronics. Scanning tunneling microscopy (STM) was therefore employed to examine adsorption and electronic properties of **3a** on the basal plane of graphite.

Results and Discussion

Synthesis. The synthesis of the bis-HBCs **3a** and **3b** is outlined in Scheme 1. The key step was the reductive coupling of the bromo-substituted HBCs **11a** and **11b**, respectively, under Yamamoto conditions. The syntheses of **11a** and **11b** are described elsewhere.[10] Thus, reaction of **11a** with [Ni(COD)$_2$] in the presence of 2,2′-bipyridyl and COD in toluene afforded bis-HBC **3a** in 85% yield after recrystallization from tetrachloroethane.[11]

The field desorption mass spectrum of **3a** shows a signal at *m*/*z* 2726.7 of M(**3a**)$^+$, which unequivocally proves the coupling of **11a** under these conditions. Due to the low solubility of this compound in common organic solvents at room temperature, high-boiling solvents, such as tetrachloroethane or 1,4-dichlorobenzene, were necessary to obtain ^{1}H NMR spectra of **3a.** The aryl protons (1,4-dichlorobenzene, 140 °C) at the positions adjacent to the junction of the HBC unit (H-1, H-1′, H-3, H-3′) give a single peak at $\delta = 9.41$ (4 H), while the remaining aryl protons appear at $\delta = 8.99$ (4 H), 8.81 (4 H), 8.76 (4H), 8.69

(7) Iyer, V. S.; Wehmeier, M.; Brand, J. D.; Keegstra, M. A.; Müllen, K. *Angew. Chem., Int. Ed. Engl.* **1997**, *36*, 1604.

(8) Birks, J. B. *Photophysics of Aromatic Molecules*; Wiley: London 1970.

(9) Harris, D. C.; Bertolucci, M. D. *Symmetry and Spectroscopy: An introduction to vibrational and electronic spectroscopy*; Dover Academic Press: New York, 1989.

(10) Ito, S.; Wehmeier, M.; Brand, J. D.; Kübel, C.; Epsch, R.; Rabe, J. P.; Müllen, K. *Chem. Eur. J.*, in press.

(11) Yamamoto, T.; Morita, A.; Miyazaki, Y.; Maruyama, T.; Wakayama, H.; Zhou, Z.; Nakamura, Y.; Kanbara, T.; Sasaki, S.; Kubota, K. *Macromolecules* **1992**, *25*, 1214.

(12) (a) Cassar, L. *J. Organomet. Chem.* **1975**, *93*, 253. (b) Dieck, H. A.; Heck, F. R. *J. Organomet. Chem.* **1975**, *93*, 259. (c) Sonogashira, K.; Tohda, Y.; Hagihara, N. *Tetrahedron Lett.* **1975**, 4467.

(13) Kovacic, P.; Koch, F. W. *J. Org. Chem.* **1965**, *30*, 3176.

Scheme 2. Alternative Synthesis of **3b**[a]

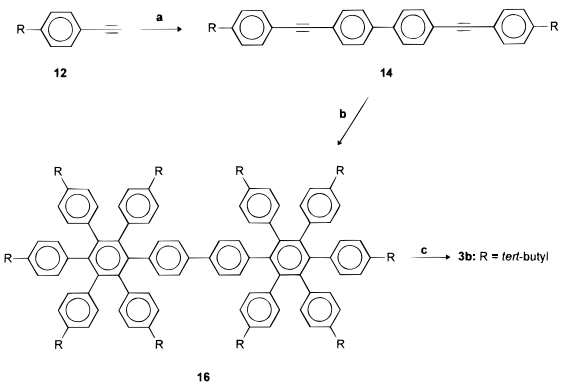

[a] Reaction conditions: (a) 4,4′-dibromobiphenyl (**13**), [Pd(PPh$_3$)$_4$], CuI, piperidine, 80 °C; (b) tetra(4-*tert*-butylphenyl)cyclopentadienone (**15**), diphenyl ether, reflux; (c) $FeCl_3$, CH_2Cl_2, room temperature.

(4H), and 8.65 (4H), respectively. The benzylic protons of the *n*-dodecyl chains exhibit broad absorptions at $\delta = 3.56$ (8 H), 3.35 (8 H), and 3.25 (4 H), respectively. The signal broadening suggests a strong aggregation of the extended HBC cores even at higher temperatures (see below). Following the above method, the *tert*-butyl substituted homologue of **3a**, **3b**, was prepared by homocoupling of **11b** in a yield of 75%.

Alternatively, **3b** was obtained by oxidative cyclodehydrogenation of the oligphenylene precursor **16** (Scheme 2).

The synthesis started with 4-*tert*-butylphenylacetylene (**12**), which was coupled with 4,4′-dibromobiphenyl (**13**) to yield **14** (81%).[12] The Diels−Alder reaction of **14** with an excess of tetra(4-*tert*-butylphenyl)cyclopentadienone (**15**) in refluxing diphenyl ether afforded **16** in a yield of 85%. Finally, **16** was cyclodehydrogenated with $FeCl_3$ in CH_2Cl_2 to furnish the target compound **3b** (81%).[13] The structure of **3b** was confirmed by field desorption mass spectrometry, which proves the loss of 24 hydrogen atoms during the course of the cyclodehydrogenation, as well as by ^{1}H NMR spectroscopy. As in the case of **3a**, the low solubility of **3b** in organic solvents at room temperature required the use of a high-boiling solvent (tetrachloroethane, 140 °C) to obtain a ^{1}H NMR spectrum. In contrast to **3a**, the resonances of **3b** appear as sharp peaks. Furthermore, the absorptions of the aromatic protons are markedly downfield shifted compared to those of **3a**. Thus, protons H-1, H-1′, H-3, and H-3′ resonate at $\delta = 10.05$ and the remaining protons resonate at $\delta = 9.66$ (4 H), 9.40 (4 H), 9.35 (4 H), 9.32 (4 H), and 9.27 (8 H). Both the significant downfield shift (i.e., a small or negligible intermolecular shielding of the aromatic cores) and the sharpness of the signals (i.e., a fast isotropic rotation of the molecules) indicate that the bulky *tert*-butyl groups prevent a pronounced aggregation of the aromatic cores of **3b** in solution.

The spacer linked bis-HBC **4** was prepared similarly to **3b** using the cycloaddition and cyclodehydrogenation sequence as shown in Scheme 3. First, the diacetylene compound **17** was coupled with 4-bromoiodobenzene (**18**) providing **19** (88%).[12] **19** was then hydrogenated to give **20** in a yield of 79%. Coupling of **20** with 4-*n*-dodecylphenylacetylene afforded diacetylene **22** in a low yield (42%).[12] Reaction of **22** with tetra(*n*-dodecylphenyl)cyclopentadienone in refluxing diphenyl ether gave the hexaphenyl derivative **24** (73%), which was finally cyclodehydrogenated to **4** by treatment with $FeCl_3$ in CH_2Cl_2 (72%).

The field desorption mass spectrum of **4** shows the clean loss of 24 hydrogen atoms from the oligophenylene precursor **24** upon cyclodehydrogenation with $FeCl_3$ without any chlorination of the aromatic core. Compared to **3a** and **3b**, **4** exhibits a fairly good solubility in various organic solvents even at room temperature. Due to the aggregation of the aromatic cores, the ^{1}H NMR spectrum of **3** shows a considerable signal broadening at room temperature. However, the signals become gradually sharper with increasing temperature. The ^{13}C NMR spectrum shows only 8 signals in the aromatic region and 17 signals in the aliphatic region.

Scheme 3. Synthesis of **4**[a]

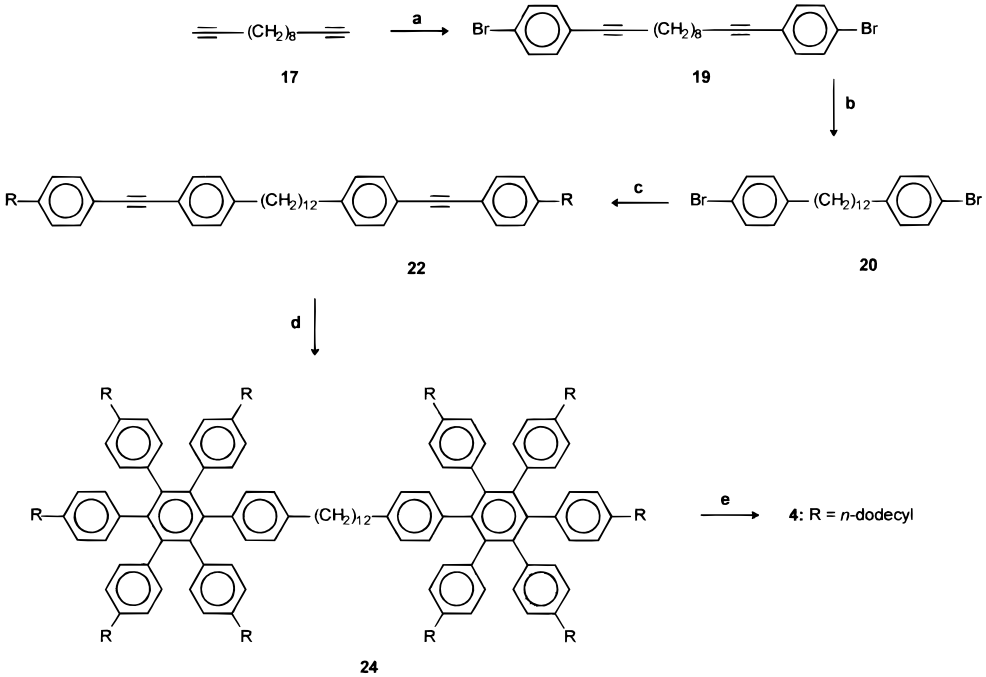

[a] Reaction conditions: (a) 4-bromoiodobenzene (**18**) [Pd(PPh$_3$)$_4$], CuI, piperidine, room temperature; (b) H_2, Pd/C, THF, room temperature; (c) 4-*n*-dodecylphenylacetylene (**21**), [Pd(PPh$_3$)$_4$], CuI, piperidine, 80 °C; (d) tetra(4-*n*-dodecylphenyl)cyclopentadienone (**22**), diphenyl ether, reflux; (e) $FeCl_3$, CH_2Cl_2, room temperature.

Table 1. Phase Transition Temperatures and Enthalpy Data (J/g in Parentheses) of **1b**, **3a**, and **4** from DSC (Measurements Are for the Second Heating Run)

system	T_m (°C)	T_i (°C)	phase width (K)	LC phase
1b	60	399	339	D_{ho}
3b	124			
4	53	370	317	D_{ho}

Figure 1. Texture of a sample of **4** between crossed polarizers at 300 °C. Magnification, 200×.

Bulk Properties. The bulk phase behavior of the new bis-HBCs **3a** and **4** was established by means of polarization microscopy and differential scanning calorimetry (DSC) as well as X-ray diffractometry. The DSC data are summarized in Table 1. **3a** shows a peak at 124 °C, which corresponds to the transition from the solid state into the mesophase, while the DSC curve of bis-HBC **4** indicates a melting point at 53 °C.

Both phase transitions are reversible with a little supercooling. The LC phase of **3a** is extraordinarily wide (317 °C) and is comparable to the one of **1b**.[2] In analogy to **1b**, the bis-HBC **4** exhibits a D_h-like texture in the mesophase which is manifested by polarization microscopy (Figure 1).

The LC columnar structure of **3a** was established by X-ray diffraction. The alkyl chain halo manifests the disordered liquid character of the mesophase of **3a**. However, the X-ray diffractogram shows that **3a** does not form a well-defined monotropic D_h mesophase. Apparently, the direct linkage of the two HBC units prevents a perfect self-organization of this compound.

The X-ray diffractogram of bis-HBC **4** proves the formation of an ordered columnar structure with a hexagonal superstructure. The intercolumnar distance was determined from the (100) reflections and amounts to 28.0 Å, the (001) reflections indicate an intramolecular distance of 3.66 Å. The (110) reflections prove the hexagonal superstructure of the columnar discotic phase. Finally, the disordered liquid character of the mesophase of **4** is revealed by the alkyl chain halo. Remarkably, the LC phase behavior of bis-HBC **4** shows only slight differences to the one of the HBC **1b**.[2]

Table 2. Gel Formation of **3b** and **4**

system	*n*-heptane	$CHCl_3$	toluene	THF
3a	3 g/L	no	5 g/L	no
4	10 g/L	no	10 g/L	no

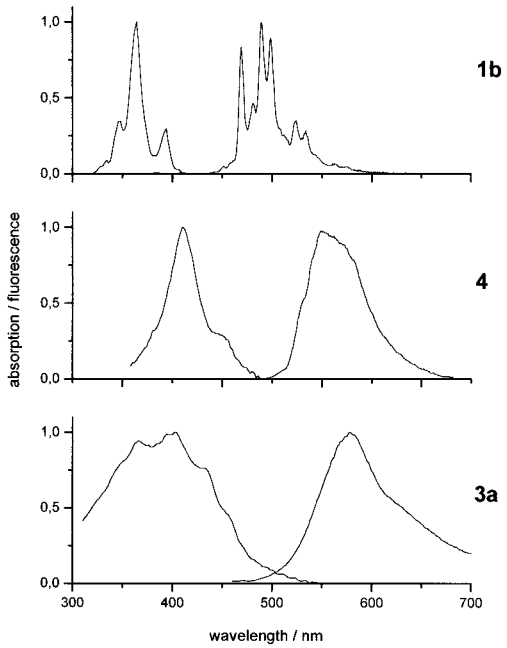

Figure 2. Absorption and fluorescence spectra of HBC **1b** and the bis-HBCs **4** and **3a**) in 1,2-dichlorobenzene at room temperature.

Gel Formation. The bis-HBC derivatives **3a** and **4** were found to form gels with certain organic solvents such as *n*-heptane and toluene, immobilizing the solvent at very low concentrations, whereas with better solvents such as chloroform and tetrahydrofuran neither **3a** nor **4** formed good gels at low concentrations. Table 2 summarizes the minimum concentrations of **3a** and **4** required for the gel-forming process.[14]

Organic gels composed of low-molecular-weight organic compounds are of interest as a novel class of organic materials that behave macroscopically as solids but contain a liquid inside.[15] Both intermolecular aggregation of the HBC cores and covalent linkage of two HBC units are responsible for the gel formation.

Fluorescence Studies in Solution. Figure 2 shows the combined absorption and fluorescence spectra of **1b**, **4**, and **3a** in 1,2-dichlorobenzene. This solvent was found to lead to a sufficient solubility of **3a**, the least soluble of the investigated compounds, such that the concentration dependence could be studied.

The spectra for **1b** are highly structured. The main peaks of absorption and fluorescence are collected in Table 3, allowing the comparison of the vibrational spacings.

The structure loss observed for the absorption spectrum of **4** is accentuated in the fluorescence spectrum, and some red-shift is observed with respect to **1b** (Figure 2). In parallel with the

(14) The gelation test was carried out as follows: A 10 mg sample of **3a** and **4**, respectively, was dissolved in an organic solvent (1, 2, 3, and 4 mL) by heating. The resulting solution was then cooled to room temperature. The gel formation was confirmed by observing that the sample did not flow when the sample was inverted.

(15) Miles, J. M. In *Developments in Crystalline Polymers*; Bassett, D. C., Ed.; Elsevier: Amsterdam, 1987; Vol. 2.

Table 3. Absorption and Fluorescence Maxima of **1b** in 1,2-Dichlorobenzene

λ (nm)	ν (cm^{-1})	$\Delta\nu(0-0)$
	Absorption	
348	28 736	3355
364	27 473	2092
394	25 381	"0"
	Fluorescence	
469	21 322	"0"
481	20 790	532
489	20 450	872
498	20 080	1242
524	19 084	2238
534	18 727	2595

broadened and red-shifted absorption, **3a** also shows a strongly red-shifted and structureless fluorescence spectrum which is independent of concentration in a range up to the maximum solubility ($\sim 5 \times 10^{-6}$ mol L^{-1}).

As **1b** is the annelated analogue of benzene, it is interesting to compare the spectra of both compounds, which have in common the high 6-fold symmetry. For benzene, this high symmetry leads to a strongly forbidden S_1 absorption and emission which is weakened by vibronic coupling.[8] Thus, the 0−0 band is absent, but vibrational progressions can be observed that are built upon "false origins" resulting from coupling with one quantum of a symmetry-reducing vibration.[8,9] The absence of the 0−0 band leads to a large energy gap between absorption and emission. The same qualitative features are observed for **1b**, and from the approximate mirror image relationship between absorption and emission, the 0−0 band can be situated around 430−435 nm, i.e., considerably red-shifted from that of benzene (at 270 nm in cyclohexane solution).[8] The comparison of the spacing of the optically active vibrations in the fluorescence spectrum of **1b** (average of 430 cm^{-1}; see Table 3) and benzene (955 cm^{-1}) leads to the conclusion that the force constant is much smaller in **1b**.[8]

The loss of structure in the absorption spectrum of **4**, as compared to **1b**, together with the close energetic similarity of the spectra indicates that the HBC moieties in **4** are not undisturbed, but probably interact weakly in an intermolecular or intramolecular way. The latter possibility may be favored given that the spectra do not depend on concentration. On the other hand, the high-temperature results for **3a** (see below) indicate strong ground-state clustering, which is probably also present for **4**. This tendency for chromophore clustering is increased in the excited state as evidenced by the further loss of structure and the red-shift of the fluorescence spectrum, which can be understood as a significant contribution of excimer fluorescence from intra- or intermolecular clusters.

The strongly broadened and red-shifted absorption of **3a** with respect to that of **1b** (Figure 3) indicates a much larger interaction between the two chromophores as compared to **4**. The fluorescence of **3a** is also strongly red-shifted and completely structureless, which suggests a large structural rearrangement prior to fluorescence or the formation of intermolecular complexes. Some large biaryl compounds are known to show polar solvent-induced excited-state charge separation. A well-known example is 9,9′-bianthryl (**8**), which exhibits dual fluorescence in polar solvents with a structured excitonic component and a red-shifted charge-transfer (CT) component.[16,17] Even larger biaryls with solvent polarity effects on the fluorescence are biperylenyl[18,19] and bibenzpyrenyl. The fact that the unstructured fluorescence is virtually not red-shifted for **3a** in solvents of different polarity such as toluene (maximum at 577 nm), 1,2-dichlorobenzene (578 nm), and benzonitrile (579 nm), however, leads to the conclusion that charge separation is not involved in this case.

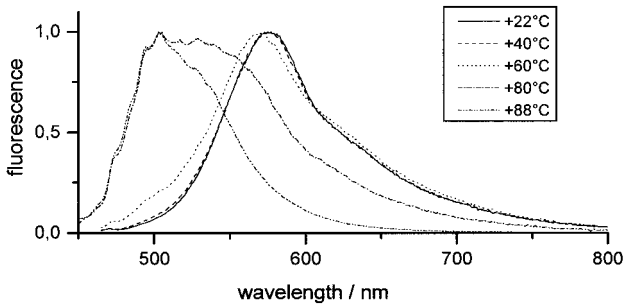

Figure 3. Fluorescence spectra of bis-HBC **3a** in 1,2-dichlorobenzene at elevated temperatures as indicated.

The nature of the relaxation coordinate that leads to the strongly red-shifted spectrum of **3a** was further investigated using high-temperature fluorescence spectroscopy (Figure 3). As evident from the spectra, an initial temperature increase does not change the structureless and red-shifted appearance of the spectra. Only at 60 °C, some additional blue fluorescence component appears which gains importance and is the major contribution at 88 °C. Some vibronic structure is visible, especially on the blue major side. This temperature dependence indicates that at room temperature the emitting species are not monomers of **3a**, but aggregates (dimers or higher clusters); further, from the lack of temperature dependence between 22 and 40 °C, and the observed concentration independence, it can be concluded that the equilibrium is totally in favor of the aggregates at room temperature. From the structuring of the fluorescence spectrum at high temperatures, a vibronic progression with a spacing of $\sim$430 cm^{-1} can be analyzed and compared to that of **1b**, which shows a similar average spacing of 430 cm^{-1} (Table 3). The first prominent shoulder is situated at 473 nm, to be compared with the first prominent band of **1b** at 469 nm (Table 3). Unfortunately, the corresponding excitation spectra showed only a weak vibronic structuring which could not be analyzed. Our comparison of **1b** and **3b** therefore rests upon the fluorescence spectrum only.

If the first prominent bands of **1b** at 469 nm and **3a** at 473 nm correspond to the same quantum of a vibronic ladder, then the red-shift for **3a** can be used to extract a rough estimate of the mutual electronic interaction between the two HBC moieties in **3a**. According to the Förster exciton model, this interaction will red-shift both absorption and fluorescence spectra. A similar analysis has been described for bianthryl and biperylenyl,[18] with the experimental red-shift (exciton interaction) for bianthryl amounting to $\sim$0.13 eV. The exciton splitting for **3a** is calculated on this basis to be very small ($\sim$0.02 eV). A possible reason for this small interaction may be the large size of the HBC moieties, which results in a large distance of the interacting transition dipoles and in small molecular orbital coefficients and hence small interaction energies.

Another relevant aspect concerns the angle of torsion about the inter-ring bond, which results from the interplay of the steric hindrance and the resonance interaction between the two HBC moieties in **3a.** This is usually different for ground and excited

(16) Rettig, W.; Paeplow, B.; Herbst, H.; Müllen, K.; Desvergne, J.-P.; Bouas-Laurent, H. *New J. Chem.* **1999**, *23*, 453.
(17) Rettig, W.; Zander, M. Ber. Bunsen-Ges. *Phys. Chem.* **1983**, *87*, 1143.
(18) Dobkowski, J.; Rettig, W.; Paeplow, B.; Koch, K. H.; Müllen, K.; Lapouyade, R.; Grabowski, Z. R. *New J. Chem.* **1994**, *18*, 525.
(19) Zander, M.; Rettig, W. *Chem. Phys. Lett.* **1984**, *110*, 602.

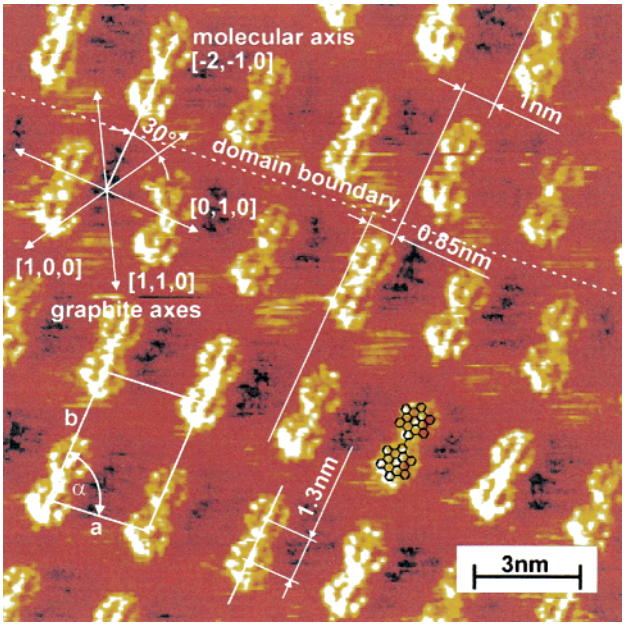

Figure 4. STM current image at constant height of a monolayer of **3a** at the interface between the basal plane of HOPG and an organic solution. The positions of the aromatic disks can be assigned to areas of high tunneling currents, which appear bright, whereas the darker regions are attributed to the alkyl side chains giving rise to a lower tunneling probability.[20] The chemical formula for the aromatic core is superimposed on the STM image and gives a better impression of the molecule's orientation and the associated contrast. Tip bias, +1.1V; current set point, 180 pA; scan rate, 976 nm/s.

states of a biaryl molecule. In the case of substituted biphenyls, planar model compounds enabled a quantitative fluorescence conformational analysis in both ground and excited states,[20] with the result that biphenyls are completely planarized in the excited state, while they are somewhat twisted in the ground state. Although such a detailed analysis is not possible here, the vibronic structure observed in the high-temperature fluorescence spectrum of **3a** (Figure 3) is consistent with an excited-state flattening and partial rigidization of the carbon skeleton in this case, too. The molecular modeling calculations reported below indicate, however, that the planarization forces are considerably weaker than for biphenyl. This is in line with the small exciton splitting as concluded above.

Scanning Tunneling Microscopy. 3a was investigated in monolayers, self-assembled at the interface between the basal plane of HOPG and a solution in 1,2,4-trichlorobenzene. Figure 4 displays a STM current image at a resolution that allows one to clearly identify two aromatic moieties per molecule.[21]

Each exhibits typically one bright spot in the middle which is surrounded by a ringlike pattern; the distance between adjacent center spots is 1.3 nm, which corresponds to the distance between the aromatic centers within one biaryl molecule. As one would expect, the submolecular patterns in the aromatic regions are symmetric with respect to the long molecular axis, and in cases of lower contrast, the patterns are smeared out into stripes with the molecule's symmetry maintained. The alkyl chains are not resolved, indicating a high conformational mobility at room temperature.

Since the structure of the isolated molecule **3a** is far from planar, one may wonder about its shape on a solid substrate.

(20) Maus, M.; Rettig, W.; Bonafoux, D.; Lapouyade, R. *J. Phys. Chem. A* **1999**, *103*, 3388.

(21) Smith, D. P. E.; Hörber, J. K. H.; Binnig, G. *Science* **1989**, *245*, 43. Lazzaroni, R.; Calderone, A.; Brédas, J. L.; Rabe, J. P. *J. Chem. Phys.* **1997**, *107*, 99.

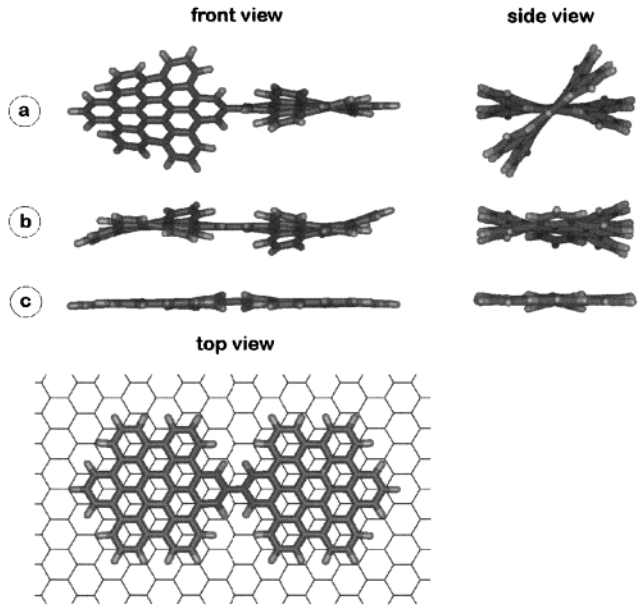

Figure 5. Molecular modeling results for **3a**: (a) the global energy minimum structure of the isolated molecule, (b) the minimum structure of the isolated molecule under the constraint of a torsion angle of 0°, and (c) the molecule on the basal plane of graphite.

However, STM imaging does not provide this information unambiguously; therefore, energy minimization calculations based on a pcff force field approach have been carried out. They reveal that the HBC disks are bent into saddlelike structures with a torsion angle of 46° between them (Figure 5).[22] The difference in energy between this minimum structure and a minimized geometry with a restrained torsion angle of 0° is 5.5 kcal/mol, indicating a rather shallow shape of the potential surface. For comparison, the benzene rings of the biphenyl molecule are rotated relative to each other by 36°, and the structure with the restrained angle of 0° is 1.6 kcal/mol higher in energy.

When **3a** is adsorbed to graphite, the aromatic moieties are flattened (Figure 5) and the gain in energy relative to the global minimum of the isolated molecule is calculated to be ~120 kcal/mol, which is more than 1 order of magnitude larger than the difference in energy between the 0 and 46° conformation. Even though the major parts of the aromatic cores lie flat on the graphite substrate, the torsion angle in this arrangement is 27.5° and the participating atoms protrude out of plane. Furthermore, the minimization has shown that the aromatic regions of the adsorbed molecule orient like additional graphene segments on the substrate no matter what the starting position of the molecule relative to the graphite substrate was.

Coming back to the experimental results, Figure 4 shows that the molecules pack along rows. Comparison with the orientation of the underlying graphite lattice indicates that the aromatic cores of the adsorbate molecules are oriented like additional graphene layers to the graphite substrate. As illustrated in Figure 6, this results in a 30° angle between the long molecular axis and a zigzag row in graphite (graphite axis).

In such a configuration, the packing of the alkyl side chains parallel to the graphite axes is easily possible and agrees with

(22) The torsion angle is defined by the two carbons forming the single bond between both aromatic regions plus the next two carbons to the left and to the right of the single bond, which are part of the adjacent benzoic subunits. Due to the warping of the aromatic moieties, the given torsion angle does not represent the angle between the two aromatic planes. However, this definition of the torsion angle is quite useful in order to get an impression to what degree the whole structure is distorted.

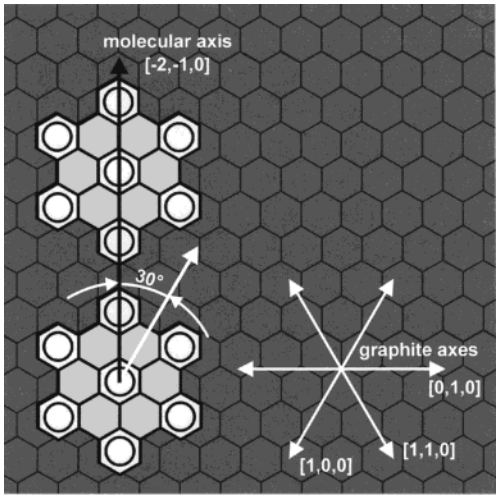

Figure 6. Schematic view of the proposed orientation of **3a** with respect to the underlying graphite substrate. The long molecular axis forms an angle of 30° with the zigzag rows in graphite.

their favored orientation, as observed for other molecules containing long alkyl chains.[23−25] Due to the anisotropic shape and the size of **3a**, the alignment of its aromatic region with respect to the underlying graphite could be resolved unambiguously. According to the present STM data and the force field-based minimizations, the major driving force for the observed orientation with respect to the graphite substrate can be attributed to the interaction between the aromatic core and the substrate underneath. Even though the alkyl side chains are in a favorable position relative to graphite, they are probably not dominating the aromatic orientation. Due to their distance to each other, a tight, crystalline packing of the alkyl parts is not possible, and one can understand that due to their flexibility their images are smeared out in the STM.

The unit cell's parameters of the spontaneously formed 2D crystal are $|\vec{a}| = 2.9 \pm 0.1$ nm, $|\vec{b}| = 4.0 \pm 0.1$ nm, $\alpha = 85 \pm 2°$, and $A = 11.5 \pm 0.7$ nm^2, with one molecule of **3a** per unit cell. This value is larger than the spatial requirements for a single molecule lying flat on a surface (foot print), which is approximately 9−10 nm^2 based on the van der Waals radii. The remaining area provides a certain degree of freedom for the flexible alkyl chains to move thermally; it also provides space to be filled to some extent by solvent molecules. This picture is consistent with molecular dynamics (MD) calculations, based on the same pcff force field approach mentioned above. The calculations indicate that the alkyl chains are adsorbed to graphite, however, not in straight all-trans conformations but rather bent at certain positions along the carbon backbone, which allows the alkyl chains to fit into the unit cell without leaving too much empty space on the surface. The resulting molecular packing exhibits neither any significant chain interdigitation nor crystallization.

Finally, small coexisting areas of a second polytype with the same occupied area per molecule (within the experimental error) were observed (Figure 4, upper right corner). Here, the molecular rows are shifted relative to each other as indicated in the STM image. Still, the orientation of the aromatic disks with respect to the underlying graphite remains the same.

(23) Rabe, J. P.; Buchholz, S. *Science* **1991**, *253*, 424.
(24) Claypool, Ch. L.; Faglioni, F.; Goddard, W. A., III; Gray, H. B.; Lewis, N. S.; Marcus, R. A. *J. Phys. Chem. B* **1997**, *101*, 5978.
(25) Strawasz, M. E.; Sampson, D. L.; Parkinson, B. A. *Langmuir* **2000**, *16*, 2326.

Chart 4

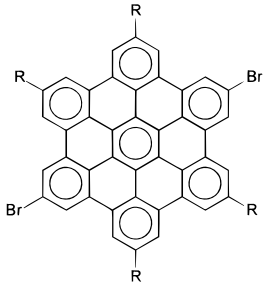

25: R = *n*-alkyl, *tert*-butyl

Conclusions

Following the chemical functionalization of HBC, this exciting molecule can now be used as a building block of more complex π-structures and a broad chemistry of "superbenzene" can be developed. The size of the resulting molecular objects becomes a key feature, with the opportunity of single-molecule investigation by STM as an important consequence. Self-assembly at the interface between the basal plane of graphite and an organic solution allowed crystallization of **3a** epitaxially in different 2D modifications. Submolecularly resolved STM in situ revealed a contrast, which reflects the structure of the aromatic parts of the molecule, and which shows that the aromatic moieties are oriented like a graphene layer in graphite.

Benzene rings are well known to serve as subunits not only of oligomers such as biphenyl or oligophenyls but also of structurally related polymers such as polyparaphenylene. Having available para-disubstituted HBCs, like **25**[10] (Chart 4), we have now synthesized polyarylenes and polyarylenealkylenes from HBC building blocks[26] and considered the interplay of intra- and intermolecular $\pi-\pi$-interactions.

Experimental Section

General Information. All reactions were carried out under an atmosphere of argon with freshly distilled solvents under anhydrous conditions. Melting points were determined on a micro melting point apparatus and are uncorrected. NMR spectra were recorded at ambient or specified temperatures on Varian Gemini 2000, Bruker AM 300, or Bruker AMX 500 instruments and calibrated with the solvent as the internal reference. Mass spectra were recorded on VG TRIO 2000 EI or ZAB2-SE-FPD equipment. Absorption spectra were recorded on a ATI Unicam UV4 UV−visible spectrophotometer; corrected fluorescence spectra were taken on a Aminco Bowman 2 fluorometer. STM was carried out in the constant-height mode in situ at solid−liquid interfaces[23] using a homemade beetle-type low-current STM[27] interfaced to Omicron electronics (Omicron Vakuumphysik GmbH). Images were recorded with Pt/Ir tips and are presented without digital image processing. The graphite lattice was used as internal calibration standard for correcting the images for distortion and drift. For this purpose, the tunneling parameter were changed (tip bias, +0.1 V; current set point, 600 pA) in order to resolve graphite after an image of the monolayer of **3a** was recorded. Solvents were of spectroscopic quality. Elemental analyses were performed by the Institut für Organische Chemie, Johannes Gutenberg-Universität in Mainz, Germany. Molecular modeling was performed using the Software Package Discover 4.0.0 (1996) by Molecular Simulation Inc., USA with the force field pcff, nonbond interactions atom based, cutoff distance 0.95 nm, final convergence 0.001 kcal mol^{-1} Å^{-1}. The minimized structure of the isolated molecule with no alkyl side chains attached to the aromatic cores was obtained as follows: A number of different starting geometries were chosen in order to scan a sufficient area of the potential surface for local minimums. All minimizations started from planar aromatic structures,

(26) Watson, M.; Müllen, K., to be published.
(27) Samori, P.; Francke, V.; Müllen, K.; Rabe, J. P. *Chem. Eur. J.* **1999**, *5*, 2312.

differing only in the above-defined torsion angle and led to various minimums on the potential surface. The geometries with a starting torsion angle of 50, 60, and 70°, respectively, resulted in the same minimum with the torsion angle of 46°, which could be identified as the global minimum.

2,2′-Bis(5,8,11,14,17-penta-*n*-dodecylhexa-*peri*-hexabenzocoronenyl) (3a). To a deoxygenated mixture of 1,5-cyclooctadiene (3 mL) in toluene (25 mL), [Ni(COD)$_2$] (116 mg, 0.422 mmol) and 2,2′-dipyridyl (68 mg, 0.42 mmol) were added. After the mixture was stirred at room temperature for 1 h, a deoxygenated solution of **11a** (501 mg, 0.347 mmol) in toluene (50 mL) was added. The resulting mixture was heated at 60 °C for 20 h. The mixture was allowed to cool to room temperature; the precipitated crystals were collected by filtration and washed with CH_2Cl_2. Recrystallization from tetrachloroethane afforded pure **3a** as yellow crystals (400 mg, 85%): mp 124 °C; ^{1}H NMR (500 MHz, $C_2D_2Cl_4$, 140 °C) δ 8.57 (br, 4 H), 8.26 (br, 4 H), 8.22 (br, 8 H), 8.07 (br, 4 H), 7.95 (br, 4 H), 3.11 (br, 8 H), 2.95 (br, 8 H), 2.71 (br, 4 H), 2.09 (br, 8 H), 2.05 (br, 8 H), 1.89−1.17 (m, 184 H), 0.94 (br, 18 H), 0.83 (br, 12 H); ^{1}H NMR (500 MHz, 1,4-dichlorobenzene-d_4, 140 °C) δ 9.41 (br, 4 H), 8.99 (br, 4 H), 8.81 (br, 4 H), 8.76 (br, 4 H), 8.69 (br, 4 H), 8.65 (br, 4 H), 3.56 (br, 8 H), 3.35 (br, 8 H), 3.25 (br, 4 H), 2.54 (br, 8 H), 2.42 (br, 8 H), 2.26 (br, 4 H), 2.17−1.46 (m, 92 H), 1.19 (br, 18 H), 1.08 (br, 12 H); IR (KBr) ν 2919, 2850, 1610, 1467, 858, 852 cm^{-1}; UV−vis ($CHCl_3$) λ_{max} (lg ϵ) 279 (4.83 sh), 323 (4.76 (sh), 344 (4.94 sh), 365 (5.05), 395 (5.06), 431 (4.79 sh), 453 nm (4.40 sh); MS (FD) *m*/*z* (%) 2726.7 (100) [M$^+$]. Anal. Calcd for $C_{204}H_{274}$ (2726.15): C, 89.87; H, 10.13. Found: C, 89.35; H, 9.79.

4,4′-Di(4-*tert*-butylphenylethinyl)biphenyl (14). At room temperature, **13** (5.0 g, 16.00 mmol) was added to a solution of [Pd(PPh$_3$)$_4$] (1.84 g, 1.60 mmol) and CuI (0.61 g, 3.20 mmol) in piperidine (300 mL). After being stirred for 20 min, **12** (7.59 g, 48.00 mmol) was added and the mixture was heated to 80 °C for 6 h. After the reaction mixture had been allowed to cool to room temperature, the precipitate was filtered off and washed with piperidine. Recrystallization from tetrachlorethane gave pure **14** as off-white crystals (6.04 g, 81%): mp 181 °C; ^{1}H NMR (500 MHz, $C_2D_2Cl_4$, 100 °C) δ 7.57 (s, 8 H), 7.47 (m, 4 H), 7.36 (m, 4 H), 1.33 (s, 18 H); ^{13}C NMR (125 MHz, $C_2D_2Cl_4$, 100 °C) δ 152.27, 140.33, 132.47, 131.86, 127.17, 125.68, 123.41, 120.68, 91.19, 89.21, 35.07, 31.54; MS (FD) *m*/*z* (%) 466.4 (100) [M$^+$]. Anal. Calcd for $C_{36}H_{34}$ (466.67): C, 92.66; H, 7.34. Found: C, 92.76; H, 7.31.

4,4′′′′′-Di-*tert*-butyl-2′,3′,5′,6′,2′′′′,3′′′′,5′′′′,6′′′′-octa(4-*tert*-butylphenyl) sexiphenyl (16). A mixture of **14** (0.5 g, 1.07 mmol) and **15** (1.56 g, 2.57 mmol) in diphenyl ether (10 mL) was heated at reflux for 3 h. The reaction mixture was then cooled to 50 °C and ethanol (80 mL) was added. Filtration of the precipitate and washing with ethanol afforded analytically pure **16** as a white microcrystalline powder (1.48 g, 85%): mp 221 °C; ^{1}H NMR (500 MHz, $CDCl_3$) δ 6.85 (m, 4 H), 6.77 (m, 24 H), 6.65 (m, 20 H), 1.07 (s, 90 H); ^{13}C NMR (125 MHz, $CDCl_3$) δ 147.55, 147.39, 147.31, 140.66, 140.47, 140.23, 139.53, 139.31, 137.98, 137.91, 137.32, 131.89, 131.12, 131.05, 124.60, 123.17, 122.99, 122.95, 34.05, 34.01, 31.22, 31.18; MS (FD) *m*/*z* (%) 1627.5 (100) [M$^+$]. Anal. Calcd for $C_{124}H_{138}$ (1628.46): C, 91.46; H, 8.54. Found: C, 91.30; H, 8.45.

2,2′-Bis(5,8,11,14,17-penta-*tert*-butylhexa-*peri*-hexabenzocoronenyl) (3b). **Method A. 3b** was prepared similarly to **3a** by heating **11b** (50 mg, 0.0566 mmol), 1,5-cyclooctadiene (0.48 mL), [Ni(COD)$_2$] (18.68 mg, 0.0566 mmol), and 2,2′-dipyridyl (10.60 mg, 0.0679 mmol) for 48 h in toluene (8 mL). Recrystallization of the crude product from 1-methylnaphthalene furnished pure **3b** as a yellow microcrystalline powder (37.50 mg, 75%).

Method B. Anhydrous $FeCl_3$ (0.62 g, 3.86 mmol) was added to a solution of **16** (0.5 g, 0.307 mmol) in CH_2Cl_2 (250 mL). The resulting green reaction mixture was stirred for 2 h at room temperature and then quenched with MeOH (10 mL). The precipitate was filtered off and washed with 5 N hydrochloric acid and MeOH. The crude material was recrystallized twice from 1-methylnaphthalene affording pure **3b** (405 mg, 81%): mp >300 °C; ^{1}H NMR (500 MHz, $C_2D_2Cl_4$, 140 °C) δ 10.05 (s, 4 H), 9.66 (s, 4 H), 9.40 (s, 4 H), 9.35 (s, 4 H), 9.32 (s, 4 H), 9.27 (br, 8 H), 1.88 (s, 36 H), 1.83 (s, 36 H), 1.82 (s, 18 H); MS (FD) *m*/*z* (%) 1603.30 (100) [M$^+$]. Anal. Calcd for $C_{124}H_{114}$ (1604.27): C, 92.84; H, 7.16. Found: C, 92.34; H, 7.05.

1,12-Di(4-bromophenyl)dodeca-1,11-diyne (19). To a solution of **18** (10.0 g, 35.4 mmol), CuI (161 mg, 0.847 mmol), and [Pd(PPh$_3$)$_4$] (931 mg, 0.805 mmol) in piperidine (150 mL) was added **17** (2.62 g, 16.1 mmol). The resulting mixture was stirred at room temperature for 3 h. The reaction mixture was poured into NH_4Cl solution and extracted with CH_2Cl_2. The organic layer was washed with NH_4Cl solution and water and then dried ($MgSO_4$). After the solvent was removed in vacuo, the residue was purified by column chromatography on silica gel with $CH)_2Cl_2$/petroleum ether (1/5) to afford **19** as colorless plates (6.70 g, 88%): mp 87.5 °C; ^{1}H NMR (200 MHz, $CDCl_3$) δ 7.40 (d, J = 8.4 Hz, 4 H), 7.24 (d, J = 8.4 Hz, 4 H), 2.39 (t, J = 6.8 Hz, 4 H), 1.71−1.28 (m, 12 H); ^{13}C NMR (50 MHz, $CDCl_3$) δ 133.49, 131.88, 123.59, 122.03, 92.18, 80.16, 29.49, 29.35, 29.09, 19.92; IR (KBr) ν = 2929, 2851, 1484, 1463, 1454, 1392, 1066, 1010, 823, 521 cm^{-1}; MS (FD) *m*/*z* (%) 472.1 (100) [M$^+$]. Anal. Calcd for $C_{24}H_{24}Br_2$ (472.02): C, 61.04; H, 5.12; Br, 33.84. Found: C, 61.06; H, 5.01; Br, 33.50.

1,12-Di(4-bromophenyl)dodecane (20). A mixture of **19** (6.00 g, 12.7 mmol) and palladium on activated carbon (10%, 1.83 g) in THF (600 mL) was stirred at room temperature for 2 h under an atmosphere of hydrogen. After the catalyst had been removed by filtration, the solvent was removed under reduced pressure. The residue was purified by column chromatography on silica gel (CH_2Cl_2/petroleum ether 1/20) affording **20** as colorless plates (4.85 g, 79%): mp 40.0 °C; ^{1}H NMR (500 MHz, $CDCl_3$) δ 7.36 (d, J = 8.4 Hz, 4 H), 7.02 (d, J = 8.4 Hz, 4 H), 2.53 (t, J = 7.5 Hz, 4 H), 1.56 (p, J = 7.5 Hz), 1.33−1.18 (m, 16 H); ^{13}C NMR (125 MHz, $CDCl_3$) δ 141.84, 131.25, 130.16, 119.25, 35.35, 31.28, 29.60, 29.53, 29.44, 29.17; IR (KBr) ν 2922, 2850, 1488, 1468, 1072, 1009, 797 cm^{-1}; MS (FD) *m*/*z* (%) 480.2 (100) [M$^+$]. Anal. Calcd for $C_{24}H_{32}Br_2$ (480.09): C, 60.01; H, 6.72,; Br, 33.27. Found: C, 61.03; H, 5.73; Br, 31.33.

1,12-Bis[4-(4-*n*-dodecylphenylethynyl)phenyl]dodecane (22). To a solution of **20** (2.00 g, 4.17 mmol), CuI (105 mg, 0.549 mmol), and [Pd(PPh$_3$)$_4$] (485 mg, 0.420 mmol) in piperidine (100 mL)was added **21** (4.54 g, 16.8 mmol). The resulting mixture was stirred at 80 °C for 24 h. The reaction mixture was poured into NH_4Cl solution. The precipitate was filtered off and washed with CH_2Cl_2. Recrystallization from *n*-heptane afforded **22** as colorless needles (1.49 g, 42%): mp 117.5 °C; ^{1}H NMR (500 MHz, $CDCl_3$) δ 7.41 (d, J = 8.1 Hz, 8 H), 7.13 (d, J = 8.1 Hz, 8 H), 2.59 (t, J = 7.4 Hz, 8 H), 1.59 (p, J = 7.4 Hz, 8 H), 1.34−1.19 (m, 52 H), 0.87 (t, J = 6.9 Hz, 6 H); ^{13}C NMR (125 MHz, $CDCl_3$) δ 143.21, 131.45, 128.42, 120.65, 88.94, 35.90, 31.92, 31.24, 29.66, 29.64, 29.61, 29.57, 29.54, 29.48, 29.34, 29.25, 22.68, 14.10; IR (KBr) ν 2920, 2847, 1516, 1469, 842, 816, 803 cm^{-1}; MS (FD) *m*/*z* (%) 858.4 (100) [M$^+$]. Anal. Calcd for $C_{64}H_{90}$ (858.70): C, 89.44; H, 10.56. Found: C, 89.40; H, 10.58.

1,12-Bis{4,4′-bis[penta(4-*n*-dodecylphenyl)phenyl]phenyl}-dodecane (24). A mixture of **22** (1.01 g, 1.18 mmol) and **23** (2.46 g, 2.33 mmol) in diphenyl ether (5 mL) was heated at reflux for 20 h. After cooling to room temperature, the mixture was chromatographed on silica gel with CH_2Cl_2/petroleum ether (1/9) to afford **5** as pale yellow crystals (2.45 g, 73%): mp 38.5 °C; ^{1}H NMR (500 MHz, $CDCl_3$) δ 6.64 (d, J = 8.1 Hz, 24 H), 6.59 (d, J = 8.1 Hz, 24 H), 2.32 (t, J = 7.5 Hz, 24 H), 1.37 (p, J = 7.5 Hz), 1.31−1.06 (m, 196 H), 0.87 (t, J = 6.9 Hz, 30 H); ^{13}C NMR (125 MHz, $CDCl_3$) δ 140.29, 139.02, 138.30, 131.41, 126.44, 35.36, 31.94, 31.24, 29.87, 29.77, 29.75, 29.69, 29.62, 29.56, 29.39, 29.02, 28.89, 28.86, 22.69, 14.09; IR (KBr) ν 2956, 2925, 2852, 1516, 1467, 1456, 1021, 834, 721 cm^{-1}; MS (FD) *m*/*z* (%) 2919.4 (100) [M$^+$]. Anal. Calcd for $C_{216}H_{322}$ (2918.53): C, 88.88; H, 11.12. Found: C, 88.76; H, 11.12.

1,12-Bis[2,2′-bis(5,8,11,14,17-penta-*n*-dodecylhexa-*peri*-hexabenzocoronenyl)]dodecane (4). To a stirred solution of **24** (1.01 g, 0.346 mmol) in CH_2Cl_2 (200 mL), a solution of $FeCl_3$ (13.2 g, 81.1 mmol) in nitromethane (30 mL) was added dropwise. A stream of argon was bubbled during the reaction mixture throughout the reaction. After being stirred for a further 30 min, the reaction was quenched with MeOH (30 mL). The resulting mixture was poured into water and extracted with hot toluene. The organic layer was washed with water, dried ($MgSO_4$), and concentrated under reduced pressure. Purification by column chromatography on silica gel with warm toluene/petroleum ether

(1/1) afforded **4** as yellow crystals (723 mg, 72%): mp 53 °C; ^{1}H NMR (500 MHz, $C_2D_2Cl_4$, 140 °C) δ 8.38 (br, 4 H), 8.36 (br, 8 H), 8.34 (br, 4 H), 8.28 (br, 8 H), 3.10 (br, 20 H), 3.02 (br, 4 H), 2.07 (br, 24 H), 1.79−1.25 (m, 196 H), 0.90 (br, 30 H); ^{13}C NMR (125 MHz, $C_2D_2Cl_4$, 140 °C) δ 139.97, 139.88, 129.96, 129.89, 123.44, 123.38, 121.29, 119.50, 37.38, 36.94, 32.04, 32.01, 31.37, 30.22, 30.02, 29.98, 29.91, 29.83, 29.43, 29.37, 28.96, 28.81, 28.67, 22.69, 13.96; IR (KBr) ν 2953, 2921, 2850, 1610, 1583, 1466, 1372, 859, 719 cm^{-1}; UV−vis ($CHCl_3$) λ_{max} (lg ϵ) 271 (4.71 sh), 322 (4.66 sh), 357 (5.25), 368 (5.11 sh), 398 (4.71), 414 (4.36 sh), 424 nm (4.06); MS (FD) *m*/*z* (%) 2895.6 (100) [M$^+$]. Anal. Calcd for $C_{216}H_{298}$ (2894.34): C, 89.62; H, 10.38. Found: C, 89.27; H, 9.91.

JA000850E